Chemical Science

ROYAL SOCIETY OF CHEMISTRY

EDGE ARTICLE

View Article Online
View Journal | View Issue

Cite this: *Chem. Sci.*, 2023, **14**, 2935

All publication charges for this article have been paid for by the Royal Society of Chemistry

Received 6th December 2022
Accepted 14th February 2023

DOI: 10.1039/d2sc06704h

rsc.li/chemical-science

Acid-induced nitrite reduction of nonheme iron(II)-nitrite: mimicking biological Fe–NiR reactions†

Kulbir, [a] Sandip Das, [a] Tarali Devi,[c] Somnath Ghosh, [a] Subash Chandra Sahoo [b] and Pankaj Kumar *[a]

Nitrite reductase (NiR) catalyzes nitrite (NO_2^-) to nitric oxide (NO) transformation in the presence of an acid (H^+ ions/pH) and serves as a critical step in NO biosynthesis. In addition to the NiR enzyme, NO synthases (NOSs) participate in NO production. The chemistry involved in the catalytic reduction of NO_2^-, in the presence of H^+, generates NO with a H_2O molecule utilizing two H^+ + one electron from cytochromes and is believed to be affected by the pH. Here, to understand the effect of H^+ ions on NO_2^- reduction, we report the acid-induced NO_2^- reduction chemistry of a nonheme Fe^{II}-nitrito complex, $[(12TMC)Fe^{II}(NO_2^-)]^+$ (Fe^{II}–NO_2^-, **2**), with variable amounts of H^+. Fe^{II}–NO_2^- upon reaction with one-equiv. of acid (H^+) generates $[(12TMC)Fe(NO)]^{2+}$, $\{FeNO\}^7$ (**3**) with H_2O_2 rather than H_2O. However, the amount of H_2O_2 decreases with increasing equivalents of H^+ and entirely disappears when H^+ reaches ≅ two-equiv. and shows H_2O formation. Furthermore, we have spectroscopically characterized and followed the formation of H_2O_2 (H^+ = one-equiv.) and H_2O (H^+ ≅ two-equiv.) and explained why bio-driven NiR reactions end with NO and H_2O. Mechanistic investigations, using ^{15}N-labeled-$^{15}NO_2^-$ and ^2H-labeled-CF_3SO_3D (D^+ source), revealed that the N atom in the $\{Fe^{14/15}NO\}^7$ is derived from the NO_2^- ligand and the H atom in H_2O or H_2O_2 is derived from the H^+ source, respectively.

Nitric oxide (NO), a critical biological component, participates in numerous bio-physiological processes such as neurotransmission, vascular regulation, inhibiting platelet aggregation, and immune response to multiple infections at nanomolar concentration.[1] Also, NO is known to be involved in plant growth and development.[2] NO meagerness may cause pathogenic effects such as atherosclerosis, diabetic hypertension, *etc.*[3] However, at micromolar concentrations, NO is highly toxic and utilized for immune defense against harmful pathogens,[4] in addition to its oxidized species, *i.e.*, peroxynitrite ($ONOO^-$)[5] or/nitrogen dioxide ($^{\bullet}NO_2$).[6] In contrast to the immune response towards pathogens, oxidized NO species also show various toxicological actions in biological systems.[5b,7]

Hence, sensible production of NO is required to maintain physiological homeostasis and is usually achieved by two metalloenzymes, *i.e.*, NO synthases (NOSs)[8] and/or nitrite reductases (NiRs).[8a,9] NOS enzymes are heme-proteins that generate NO by catalyzing the conversion of L-arginine to L-citrulline under aerobic conditions.[8b,c] However, under ischemia and hypoxic conditions, the suppression of NOS activity results in the decrease of NO generation. Under such conditions, NO_2^- works as an active NO source in biological systems, generating NO in acid-induced NO_2^- reduction reactions.[10] Sometimes, under abnormal conditions, biochemical dysfunction may cause NO overproduction by NiRs or NOSs. Under such conditions, NO dioxygenase (NOD) enzymes available *in vivo* convert excess NO to biologically benign nitrate (NO_3^-).[11] NO_3^-, the product of the NOD reaction, serves as a critical component of NO_2^- generation and a precursor to the biological NO cycle.[12] In humans, commensal bacteria in the oral cavity play a vital role in converting NO_3^- to NO_2^-.[12a] Bacteria reduce NO_3^- to NO_2^- *via* an OAT reaction mediated by molybdenum-based NR enzymes.[13] The interconversion of NO_3^- to/NO_2^-/to NO (or *vice versa*) is the critical step of the denitrification process.[14] *In vivo* studies have proven that NO_2^- is a fundamental source of NO in mammalian or bacterial systems, an intermediate species of the biological nitrogen cycle (NO_3^- → NO_2^- → NO → N_2O → N_2).[14] At the bio-physiological level, NO_2^- gets reduced to NO, primarily by globins[15] or by acid-catalyzed NO_2^- reduction in the stomach[16,17] or by Fe/Cu-NiR enzymes/cytochrome c oxidase (CcO)/xanthine oxidase,[18] which reduces NO_2^- to NO in the presence of two-equiv. of H^+ ions, *i.e.*,[8a,9,15]

$$NO_2^- + e^- + 2H^+ \rightarrow NO + H_2O \quad (1)$$

[a]*Department of Chemistry, Indian Institute of Science Education and Research (IISER), Tirupati 517507, India. E-mail: pankajatiisert@gmail.com; pankaj@iisertirupati.ac.in*

[b]*Department of Chemistry, Punjab University, Chandigarh, Punjab, India*

[c]*Humboldt-Universität zu Berlin, Institut für Chemie, Brook-Taylor-Straße 2, D-12489 Berlin, Germany*

† Electronic supplementary information (ESI) available. CCDC 2181978 and 2181979. For ESI and crystallographic data in CIF or other electronic format see DOI: https://doi.org/10.1039/d2sc06704h

However, few functional mimicking models were developed and investigated *in vivo*/*in vitro* to explore the mechanistic insight of microbial NiR enzymatic chemistry. Brooks and coworkers proposed the NiR activity of mammalian hemoglobin (Hb) protein under anaerobic conditions, which converts NO_2^- to NO with the formation of metHb.[19] E. T. Papish *et al.* explored the Cu-NiR chemistry and showed NO production with H_2O as a side product *via* a Cu^I–NO^+ ↔ Cu^{II}–NO intermediate in the reaction of Cu–NO_2^- with two-equiv. of H^+.[20] A heme-Fe/Cu assembly model has been developed to mimic the cytochrome c oxidase, illustrating the reversible conversion of NO_2^- to NO.[21] For the first time, Murphy and coworkers explored the explained Cu–NO_2^- reduction reaction to release NO *via* the {CuNO} intermediate and characterized it structurally.[9b,22] Patra and coworkers have mimicked NO_2^- reduction reactivity using Cu^{II}–NO_2^- with two-equiv. of H^+ and one e^-, leading to NO and H_2O molecule formation.[23] Lehnert and coworkers have explored electrocatalytic reduction using Cu^{II}–NO_2^- producing NO in aqueous media[24] and compiled the electronic structure and reactivity of the biologically relevant coordination chemistry of iron and NO.[15] In addition to acid-encouraged NO_2^- reduction to NO in different model systems. Various models have been explored for the reduction of metal-bound NO_2^- to NO *via* (i) oxygen atom transfer (OAT) caused by (R_2S)[25]/thiol (RSH)}[18a,26]/triphenylphosphine (PPh_3)[27]/vanadium chloride (VCl_3)[28] and (ii) photo-induced reactions[29] of metal–bound nitrite (M–NO_2^-).

In addition to the developments on biomimetic synthetic modeling of M–NOs/or active sites associated with NiR and/or NOS.[11d,30] Recently, Lehnert and coworkers have established the synthetic strategy for Fe–NOs,[31] and Nam and coworkers have explored the photo-induced NiR reactivity of Fe–NO_2^- to generate Fe–NOs and also stabilize Co–NOs.[32] Ford and coworkers continuously discover the NiR chemistry of various heme systems.[33] Although NiR is the key source of NO in the biological system, such reactions are not investigated extensively to characterize the intermediates and transition states of NO_2^- reduction reactions. Hence, several research groups are working to understand the proper NO_2^- reduction reaction mechanism. There are only very few reports on acid-induced NO_2^- reduction reactions to mimic NiR enzymatic reactions and understand the mechanistic aspects.[9b,29,34] In this investigation, we intend to characterize different intermediates of H^+-induced NO_2^- reduction in Fe^{II}–NO_2^- and its reaction products and then explore its mechanistic aspects. This report will focus on how different amounts of acid (H^+ ion) affect the reaction mechanism and regulate the side products in addition to NO.

Herein, we report the NO_2^- reduction chemistry of a nonheme FeII–NO_2^- complex, [(12TMC)Fe^{II}(NO_2^-)]$^+$ (**2**), bearing the 1,4,7,10-tetramethyl-1,4,7,10-tetraazacyclododecane (12TMC) ligand (Scheme 1, reaction I). Complex **2** reacts with one-equiv. of triflic acid (HSO3CF3, H^+ source) and generates the corresponding nonheme Fe–nitrosyl complex, [(12TMC)Fe(NO)]$^{2+}$({FeNO}, **3**), and H_2O_2 (Scheme 1, reactions II & III) in CH3CN at 233 K. However, upon reaction with a base (OH^-), **2** does not form **3**. Mechanistic investigations using ^{15}N-labeled-$^{15}NO_2^-$ demonstrated explicitly that the N atom in the NO moiety of **3** is derived from the NO_2^- anion and H_2O_2 by the protonation of the O atom of the NO_2^- moiety. Conversely, an increased H^+ concentration showed a significant fall in H_2O_2, which disappeared completely when the H^+ ion quantity was ≅ two-equiv. with the simultaneous formation of a substantial amount of H_2O (Scheme 1, reaction IV). To the extent of our knowledge, the present work reports the very first comparative study for the reaction of an Fe^{II}–NO_2^- complex with varying H^+ concentrations and the evidence showing the formation of H_2O_2 (one-equiv. of H^+) and H_2O (≅ two-equiv. of H^+), illustrating a new approach for NiR enzyme activity (Scheme 1).

Results and discussion

Preparation of the Fe^{II}-nitrito complex, [(12-TMC)Fe^{II}(NO_2^-)]$^+$ (2)

The initial FeII–NO_2^- complex, [(12TMC)Fe^{II}(NO_2^-)]$^+$ (**2**), was prepared by the addition of one equivalent of $NaNO_2$ in the presence of a 15-crown-5 to Fe^{II}-complex, [(12TMC)Fe^{II}($NCCH_3$)]$^{2+}$ (**1**), in CH3CN at 298 K (Scheme 1 & reaction I; also see the ESI and Experimental section (ES)). Complex **2** was further characterized by various spectroscopic measurements, including the determination of the single-crystal X-ray structure. A UV-vis absorption band (λ_{max} = 325 nm and ε = 356 M^{-1} cm^{-1}) was formed upon adding an equivalent amount of $NaNO_2$ to the CH_3CN solution of **1**, which corresponds to **2** (Fig. 1a). A characteristic peak for metal-bound NO_2^- stretching at 1270 cm^{-1} was observed in the FT-IR spectrum of **2**, which shifted to 1247 cm^{-1} when **2** was prepared using ^{15}N-labeled-nitrite ($^{15}N^{16}O_2^-$) (inset: Fig. 1a andS1; ESI†).[35] The electrospray ionization mass spectrum (ESI-MS) recorded for **2** showed a prominent ion peak at *m*/*z* 330.1, which shifted to m/*z* 331.1 when prepared with ^{15}N-labeled $Na^{15}N^{16}O_2$, and their mass and isotope distribution pattern corresponds to [(12TMC)Fe(NO_2^-)]$^+$ (calc. *m*/*z* 330.1) and [(12TMC)Fe($^{15}NO_2^-$)]$^+$ (calc. *m*/*z* 331.1), respectively (Fig. 1b and S2; ESI†). The ^{1}H-NMR spectrum of **2** showed fairly clean paramagnetic proton signals for the protons of the 12TMC ligand (Fig. S3a†), suggesting a magnetically active Fe center. The spin-state of the Fe center in **2** was determined by calculating the magnetic moment of the Fe^{II} center by Evans' method and found to be 5.19 BM, suggesting a high spin Fe^{II} ion (*S* = 2) in complex **2** (ESI,† ES, Fig. S3b). The electrochemical measurement of **2** showed

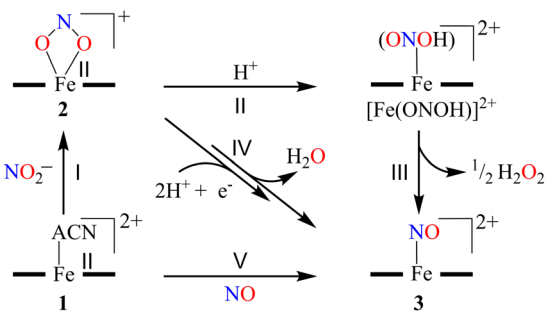

Scheme 1

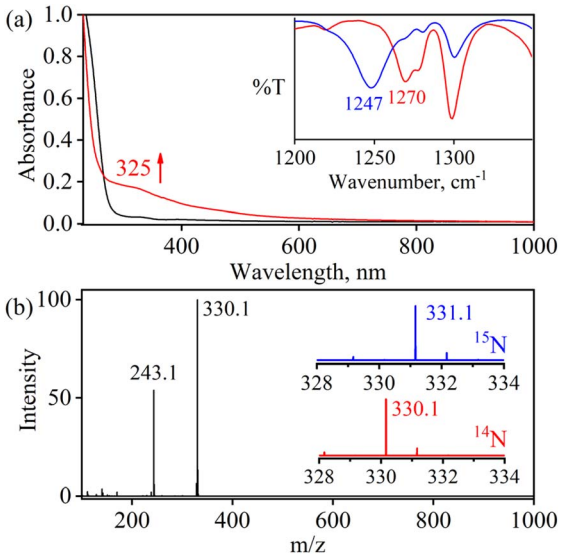

Fig. 1 (a) UV-visible spectra of **1** (0.50 mM, black line) and **2** (0.50 mM, red line) in CH_3CN under Ar at 298 K. Inset: IR spectra of **2**-$^{14}NO_2^-$ (red line) and **2**-$^{15}NO_2^-$ (blue line) in KBr. (b) ESI-MS spectra of **2**. The peak at 330.1 is assigned to $[(12TMC)Fe^{II}(NO_2^-)]^+$ (calcd *m/z* 330.1). Inset: isotopic distribution pattern for **2**-$^{14}NO_2^-$ (red line) and **2**-$^{15}NO_2^-$ (blue line).

a reversible cyclic voltammogram (redox potential + 0.56 V *vs.* $Ag/AgNO_3^-$) (ESI, Fig. S4a†). In addition to the above spectral measurements, the structural details of **2** were obtained by its single-crystal X-ray structure determination (Fig. 2). The Fe^{II} center of **2** was found to have O, O′-chelated bi-dentate NO_2^- anions in a distorted octahedral geometry (ESI,† ES, Fig. S5 and Tables 1 & 2).

The nitrite reduction reaction of the Fe^{II}–NO_2^- complex (2)

To further investigate the NO_2^- reduction chemistry of FeII–NO_2^- (**2**), we explored its reaction with different equivalents of acid (H^+ ions). When **2** was reacted with H+, we observed a visible color change from yellow to green and a new absorption band ($\lambda_{max} = 350$ nm and $\varepsilon = 1450\ M^{-1}\ cm^{-1}$), characteristic of a new species (**3**), formed over ~2 minutes in CH3CN under Ar at 233 K (Fig. 3a; ESI,† ES, and Fig. S6).[8a,9] Complex **2** was found to be very stable in CH_3CN and at 298 K as it did not show any spectral variations in the absence of H^+ (ESI,† Fig. S7a). Complex **2** was also found inert towards OH^- as it does not indicate any change in UV-vis spectra when treated with tetrabutylammonium hydroxide (ESI, Fig. S7b†), suggesting that Fe–NO_2^- reacts only with H^+. The amount of H^+ required to reduce the NO_2^- moiety was determined by spectral titration, which confirmed the ratio-metric equivalent of **2** with H^+ as 1 : 1 (ESI,† Fig. S8). The compound **3**, obtained in the reaction of **2** with H+ was determined to be an Fe–nitrosyl complex, $\{FeNO\}^7$, based on various spectroscopic characterization techniques (*vide infra*). The other product of the NO_2^- reduction using one-equiv. of H^+ was determined to be H_2O_2, in contrast to previous reports on biological NiR and NO_2^- reduction chemistry, *via* a proposed thermally unstable ONOH intermediate as reported in the literature (Scheme 1, reactions II & III).[36] However, when reacted with more than one-equiv. of H^+ (≅ two) **2** generated **3**, but the amount of H_2O_2 decreased gradually with

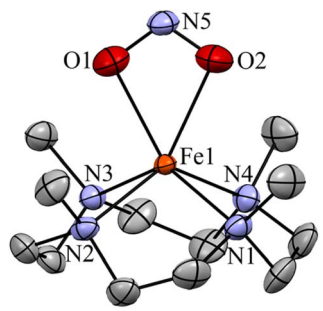

Fig. 2 Displacement ellipsoid plot (15% probability) of **2** at 100 K. Disorder C atoms of TMC, anions and H atoms have been removed for clarity.

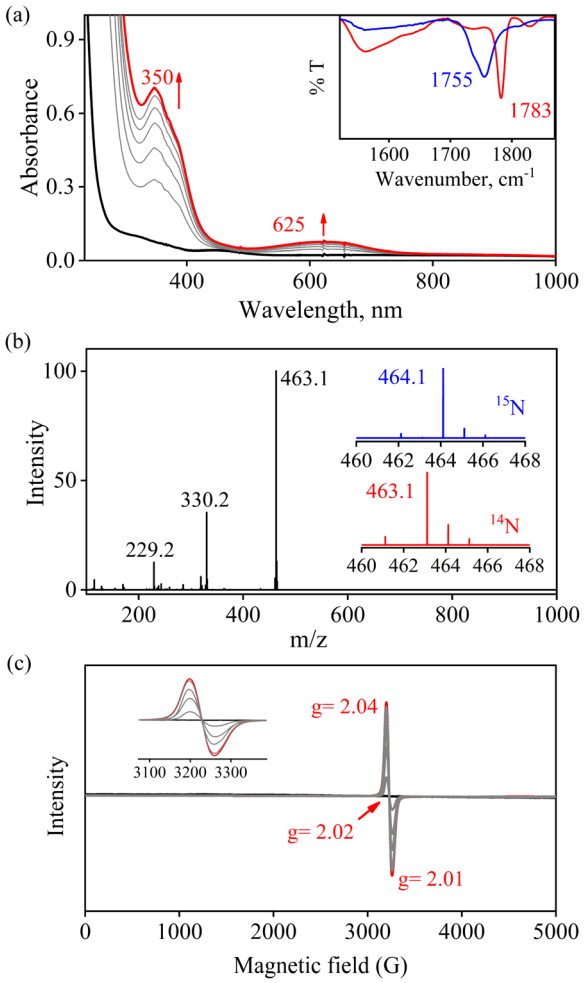

Fig. 3 (a) UV-visible spectral changes of **2** (0.50 mM, black line) upon addition of H^+ (one-equiv.) in CH_3CN at 233 K. Black line (**2**) changed to a red line (**3**) upon addition of H^+. Inset: IR spectra **3**-^{14}NO (red line) and **3**-^{15}NO (blue line) in KBr. (b) ESI-MS spectra of **3**. The peak at 463.1 is assigned to [(12TMC)FeII(NO)(OTf)]+ (calcd *m/z* 463.1). Inset: isotopic distribution pattern for **3**-14NO (red line) and **3**-15NO (blue line). (c) Time-dependent EPR spectra of the generation of **3** (red line) in the reaction of **2** and H^+ (one-equiv.) in CH_3CN at 77 K.

increasing H^+. This suggests the decomposition of H_2O_2 or utterly new chemistry in the presence of more than one-equiv. of H^+; the new product was confirmed to be H_2O by using various spectral measurements (Scheme 1, reaction IV). To the best of our knowledge, this work reports the first-ever study where the side products of NO_2^- reduction are regulated by different amounts of H^+, which opens a new pathway of acid-induced NO_2^- reduction chemistry to the scientific community.

We have performed various spectral measurements to track the products of H^+ (or D^+)-induced reduction of Fe-bound $^{14/15}NO_2^-$ in **2**. The FT-IR spectrum of **3** showed a characteristic peak for Fe-bound nitrosyl stretching at 1783 cm^{-1} ($\{Fe^{14}NO\}^7$), which shifted to 1755 cm^{-1} ($\{Fe^{15}NO\}^7$) when **3** was prepared by the reaction of ^{15}N-labeled-nitrite (**2**-$^{15}NO_2^-$) with one-equiv. of H^+ (inset, Fig. 3a and S9; ESI†). This shifting in NO stretching frequency ($\Delta = 28$ cm^{-1}) indicates that the N atom in NO moiety is derived from the $^{14/15}NO_2^-$ ligand of **2**. Similarly, the ESI-MS spectrum of **3** showed a prominent peak at *m*/*z* 463.1, [(12TMC)Fe(NO)(OTf)]$^+$ (calc. *m*/*z* 463.1), which shifted to 464.1, [(12TMC)Fe(^{15}NO)(OTf)]$^+$ (calc. *m*/*z* 464.1), when Fe^{II}–$^{15}NO_2^-$ was reacted with H^+ (Fig. 3b and S10; ESI†), specifying clearly that NO in **3** is derived from the NO_2^- moiety. The ^{1}H-NMR spectrum of **3** showed shifting in the ^{1}H-signals of the 12TMC ligand framework suggesting a paramagnetic system (ESI, Fig. S11a†).[32a,b] We determined the spin-state of the Fe centre in **3** by calculating its magnetic moment using Evans' method and found it to be 2.3 BM, suggesting a low-spin Fe center in **3** (S = 1/2) for the complex **3** (ESI, ES, and Fig. S11b†).[37] Additionally, time-dependent EPR measurements were followed for the generation of **3** in the reaction mixture of **2** + H^+. EPR measurements (77 K), performed at different time intervals, showed the formation of a new species ($g = 2.04$) (Fig. 3c), which is characteristic of the EPR signal of isolated species $\{FeNO\}^7$ (Scheme 1, reaction V), confirming the formation of low-spin **3** in the above reaction (ESI, Fig. S11c†). The electrochemical measurement of **3** showed a reversible cyclic voltammogram (redox potential + 0.36 V *vs.* Ag/$AgNO_3^-$) (ESI, Fig. S4b†). Additionally, we have determined the binding constants $K_b(Fe^{II}–NO_2^-)$ and $K_b\{(Fe(NO)\}^7$ using the Benesi–Hildebrand equation[28,38] for the generation of **2** and **3** in the reaction of $[(12TMC)Fe^{II}(CH_3CN)]^{2+}$ with NO_2^- and NO. The values were $K_b(Fe^{II}–NO_2^-) = 4.7 \times 10^2$ M^{-1} & $K_b\{(FeNO\} = 8.4 \times 10^2$ M^{-1} (ESI,† ES, and Fig. S12), which also supports the forward reaction. In addition, the yield for the formation of **3** was calculated by comparing the UV-vis absorption spectra of **3** formed in the reaction of **2** with one-equiv. of H^+ with the authentic Fe–nitrosyl complex ($\{FeNO\}^7$), prepared in a separate reaction of $[(12TMC)Fe^{II}(CH_3CN)]^{2+}$ + NO, and was found to be 95%. However, the yield decreased to 85% when the reaction was carried out using two-equiv of H^+ (ESI, ES, and Fig. S13†). Furthermore, the structural details of **3**, obtained in the reaction of **2** and H^+, were obtained by its single-crystal X-ray structure determination (ESI, ES & Fig. 4). The NO moiety showed the coordination *via* the N atom to the Fe center of **3** with the a angle of 168° (ESI, ES Fig. S14;† & Tables T1 and T2). This arrangement suggests a neutral $^{\bullet}$NO moiety with an Fe^{II} center[37,39] (further supported by BVS calculation from the crystal parameters of **3**, ESI,† ES) and can be formulated as

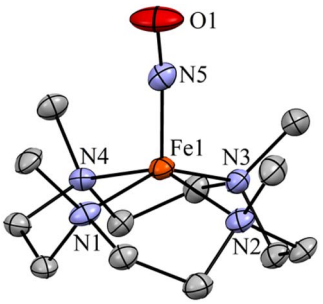

Fig. 4 Displacement ellipsoid plot (50% probability) of **3** at 100 K. Disordered C atoms of TMC, anions and H atoms have been removed for clarity.

[(12TMC)Fe^{II}(NO)]$^{2+}$; however, in this manuscript, we used Enemark–Feltham notation for **3** ($\{FeNO\}^7$).

Mechanistic investigation of NO_2^- reduction

In vivo and *in vitro* biomimetic studies on acid-induced NO_2^- reduction reactions produce NO with H_2O (as explained in the biological NiR chemistry)[34a,40] or in some cases $^{\bullet}$OH (H_2O_2)[36] or a metal hydroxide[41] and should be accomplished *via* the proposed ONOH intermediate, as reported by Murphy *et al.*,[9b] and Rose *et al.*[40g] for the biological Cu-NiR chemistry. Similarly, Fujii and coworkers also proposed a Cu(ONOH) intermediate in the acid-induced biomimetic NO_2^- reduction on the Cu^I center.[40h] Meanwhile, Shigeta *et al.*[40i] & Chen and coworkers[40j] theoretically established the presence of a Cu(ONOH) intermediate in acid-induced NO_2^- reduction. The present work elucidated how varying equivalents of H^+ ions determine the side products of Fe^{II}-bound NO_2^- reduction chemistry in addition to NO and should be accomplished by a similar proposed ONOH intermediate. In this regard, we proposed the reaction sequences, where the preliminary step of the NO_2^- reduction reaction consists of an electrophilic addition of H^+ to the NO_2^- anion of **2** and generating the suggested $[Fe–ONOH]^{2+}$ intermediate species (Scheme 2, reaction I), as proposed previously.[36,41] The presumed $[Fe–(ONOH)]^{2+}$ intermediate is believed to produce $\{FeNO\}^7$ *via* the homolytic cleavage of the ON–OH moiety, as reported in NO_2^- reduction on

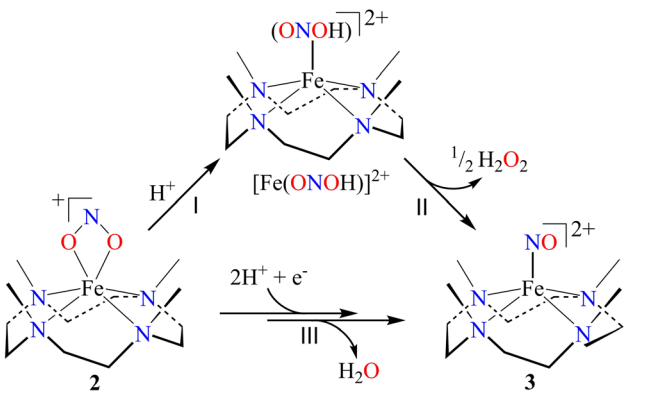

Scheme 2

the Fe^{II} center and Cu-NiR,[36,41] and $^{\bullet}OH$ ($^1/_2$ H_2O_2)[42] (Scheme 2, reaction II). In contrast, NO_2^- reduction in the presence of ≈ two-equiv. or more H^+ produced **3** with H_2O as a side product in a multiple-step reaction (Scheme 2, reaction III). This reaction is believed to occur *via* the reduction of the NO_2^- anion of **2** in the presence of two H^+, as reported in biological NiR[9b,40g] and biomimetic NO_2^- reduction[40h–j,43] reactions. The H_2O molecule may be generated either by (a) step-wise protonation of NO_2^- species of **2** as observed in biology,[40a,b] (b) acidic decomposition of H_2O_2,[44] or (c) by auto-decomposition of H_2O_2.[45]

To validate our proposed H^+-induced NO_2^- reduction chemistry mechanism, we have reacted **2** with different equivalents of H^+ and characterized all the products formed in the reaction mixture. In both the acid-induced reactions, we observed the formation of **3**. However, the side product of NO_2^- reduction changed to H_2O instead of H_2O_2 when the H^+ amount was ≥ two-equiv. (ESI,† ES). H_2O_2/& H_2O formed in the NO_2^- reduction reaction was followed/characterized and quantified using ^{1}H-NMR spectroscopic measurements. A characteristic signal for H_2O_2 (8.66 ppm, ESI,† Fig. S15a)[46] was observed in the ^{1}H-NMR spectrum of **2** with one-equiv. of H^+ in CD_3CN. Our proposal of H_2O_2 formation in one-equiv. of H^+ induced NO_2^- reduction was authenticated by comparing this spectrum with those of the authentic samples: (i) H_2O_2 plus **3** (8.66 ppm; ESI,† Fig. S15b) and (ii) H_2O_2 only (8.66 ppm; ESI,† Fig. S15c).[46] The amount of H_2O_2 in the above reaction was confirmed to be more than 50% (defining $\frac{1}{2}$ equivalent of H_2O_2 relative to **2** as 100% yield) from ^{1}H-NMR spectral measurements and using benzene as the internal standard (ESI,† ES, and Fig. S15a).[46] Time-based ^{1}H-NMR spectral measurements for the above reaction showed the gradual formation of H_2O_2 (8.66 ppm), which starts decreasing after reaching its maxima, suggesting the decomposition of H_2O_2 to H_2O (Fig. 5a).[44,45] In addition to ^{1}H-NMR, iodometric titration likewise confirmed H_2O_2 formation in the reaction of **2** with one-equiv. of H^+ which was determined to be ∼65% (ESI, ES, and Fig. S16a†) (defining 1/2 equivalent of H_2O_2 relative to **2** as 100% yield). However, no H_2O_2 was observed in iodometric titration when the reaction was carried out in the presence of two-equiv. of H^+ (ESI, ES, and Fig. S16b†).[47]

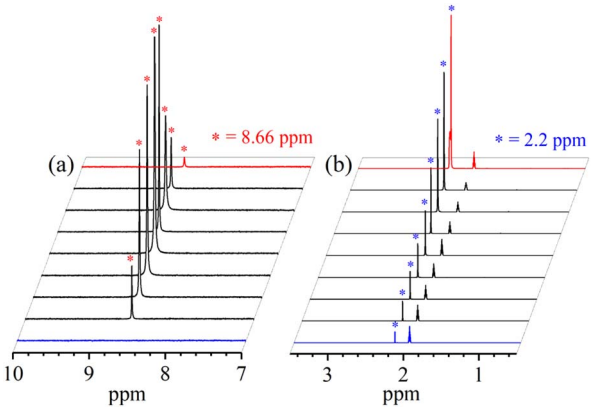

Fig. 5 1H-NMR spectrum of (a) H_2O_2 formation and (b) H_2O formation in the reaction of **2** with one-equiv. & two-equiv. of H^+ in CD_3CN recorded at different times, respectively.

Furthermore, we have also established H_2O formation in the NO_2^- reduction reaction in the presence of two-equiv. of H^+ by ^{1}H-NMR spectroscopic measurements (Fig. 5b and S15d, ESI†). To establish that H^+ is only responsible for forming ^{1}H-NMR signals at 2.2 ppm, we have explored the same reaction using CF_3SO_3D (D^+ source). Surprisingly, when the source was D^+, we did not observe the formation of the H_2O peak (at 2.2 ppm); this clearly suggests that H^+ ions are responsible for the H_2O formation in the two-equiv. of H^+ induced NO_2^- reduction (ESI, ES, and Fig. S17†). In addition, time-dependent ^{1}H-NMR spectral measurements for the reaction of **2** with two-equiv. of H^+ showed an increment in the peak of H_2O protons and a kind of first time-base measurement, further supporting our proposal of H_2O formation (Fig. 5b). However, our efforts to quantify the amount of H_2O formed in the reaction are futile; but they scientifically established the mechanistic aspect of acid-induced NO_2^- reduction in the presence of different equivalents of H^+. These results are the only example where tracking H^+-induced NO_2^- reduction products has confirmed that the variable amounts of H^+ (pH/acidic conditions) generate NO with H_2O_2 (one-equiv. of H^+) or H_2O (≥two-equiv. of H^+).

Furthermore, we attempted to characterize the proposed $[Fe–ONOH]^{2+}$ intermediate to illustrate its conversion mechanism to **3**. However, after several attempts, we failed to detect/stabilize the intermediate even at low temperature (193 K) in UV-vis & FT-IR spectroscopic measurements, suggesting a kinetically driven reaction.[48] Since metal-nitrous acid intermediates are known to be highly unstable intermediates,[34b,36,40h–j] there are only a few reports about the metal-bound nitrous acid species.[34b,40h,40j,49] However, to support our mechanistic proposal for the formation of an $^{\bullet}OH$ radical (H_2O_2) *via* the homolytic cleavage of the N–O bond, we pursued the $^{\bullet}OH$ radical trapping experiment using 2,4-di-*tert*-butylphenol (2,4-DTBP).[50] In the one-equiv. of H^+ induced NO_2^- reduction reaction, we have observed the formation of 3,5-Di-*tert*-butylcatechol (3,5-DTBC, ∼22%) and 2,4-DTBP-dimer (2,4-DTBP-D, ∼8%) with a minimal amount of nitro-2,4-DTBP (NO_2-2,4-DTBP, ∼6%) (ESI, ES, and Fig. S18 & S19†). The generation of 3,5-DTBC[51] in the above experiments undoubtedly confirmed the $^{\bullet}OH$ formation *via* the N–O bond homolysis of the ON–OH moiety. Hence, the formation of 3,5-DTBC and other products confirms the reaction sequences (Scheme 3) and supports the

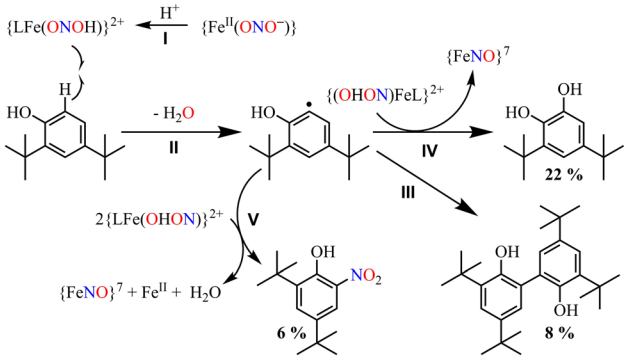

Scheme 3

presence of the $[Fe\text{-}(ONOH)]^{2+}$ intermediate in the one-equiv. of H^+ induced NO_2^- reduction reaction.

The transformation of 2,4-DTBP in the presence of one-equiv. of H^+ can be explained based on the radical coupling reaction.[51] The sequences of the 2,4-DTBP conversion are believed to be (i) the generation of the phenoxyl radical and the release of Fe–NOs by the H-atom abstraction reaction of $[Fe\text{–}ONOH]^{2+}$ from DTBP (Scheme 3, reaction I & II). After that, the phenoxyl radical either (ii) dimerizes to give 2,4-DTBP-D (Scheme 3, reaction III) or (iii) produces 3,5-DTBC upon radical coupling with another molecule of $[Fe\text{–}ONOH]^{2+}$ and releases **3** (Scheme 3, reaction IV). In some cases, NO_2-DTBP and **3** may generate in the presence of two molecules of $[Fe\text{–}ONOH]^{2+}$ and a phenoxyl radical (Scheme 3, reaction V). Also, when the above radical trapping experiments were performed using CF_3SO_3D, we observed the generation $^{\bullet}OD$-driven products of DTBC (ESI,† ES, and Fig. S20). In addition, we reacted **2**-$^{16}O^{14}N^{18}O^-$ with one equiv. of H^+ in the presence of 2,4-DTBP. Surprisingly, we observed the formation of 3,5-DTBC (^{18}OH) with $^{16}O^{14}N^{18}O$-DTBP as a side product (ESI, Fig. S21†). These experiments support that one equiv. of H^+ induced NO_2^- reduction in **2** generates **3** + H_2O_2 *via* the homolytic cleavage of the N–O bond of the ON-OH intermediate.[36]

Conclusion

The mechanistic investigation of acid-induced NO_2^- reduction became an important research topic in modern-day chemistry as it deals with NO_2^- to NO transformation, an essential signaling molecule in biosystems.[40b,52] The mechanistic aspects of NiR chemistry mediated by H^+ are still challenging to the scientific community and yet to be resolved as two different side products have been proposed to form *in vivo* and *in vitro* studies.[8a,9,16,25,30] Also, the pH/or H^+ ion concentration effect is yet to be confirmed as it affects the reaction mechanism and the side products of NO_2^- reduction reactions.[48] In this report, we have shown the reduction of NO_2^- in a nonheme Fe^{II}-nitrito complex, $[(12TMC)Fe^{II}(NO_2^-)]^+$ (**2**), to an Fe–nitrosyl complex $[(12TMC)Fe(NO)]^{2+}$, $\{FeNO\}^7$ (**3**), in the presence of different equivalents of H^+ (CF_3SO_3D, D^+ ion source), a biomimetic functional model of NiR. The structural details of $\{FeNO\}^7$ showed an axially coordinated NO moiety to the Fe center. In addition, ^{15}N-labeled $^{15}NO_2^-$ experiments confirm that the N atom of the NO moiety in **3** is derived from the NO_2^- anion of **2**. Acid-induced NO_2^- reduction of **2** showed the formation of $\{FeNO\}^7$ along with H_2O_2 or H_2O as a side product when treated with different ratios of H^+, one-equiv. or ≥two-equiv., respectively. Reports on acid-induced biomimetic NO_2^- reduction[40h,j,43] and biological NiR reactions[9b,40g,41] suggested a metal-ONOH intermediate before NO formation; hence, we believe that the H^+-induced NO_2^- reduction on the Fe^{II} center in **2** should generate **3** *via* the proposed $[Fe\text{–}ONOH]^{2+}$ intermediate and follow the NiR chemistry. The N–O bond homolysis of the proposed ONOH intermediate was supported by the observation of 3,5-DTBC-^{16} OH(^{18} OH) in $^{\bullet}OH$ radical trapping experiments using 2,4-DTBP[51] in the reaction of **2**-$ON^{16}O_2^-$($^{16}ON^{18}O^-$) with one equiv. of H^+. Also, the observation of DTBC(OD) in the presence of D^+ further supports the acid-induced reduction of NO_2^-. In addition, a significant amount of H_2O_2 formation was also confirmed using ^{1}H-NMR/or UV-vis iodometric titration along **3**.[46] However, the generation of the H_2O molecule was believed to occur either (i) by NO_2^- reduction in the presence of two-equiv. of H^+ and an electron[9b,40c,40g,40h,40j] or (ii) by the acid-induced decay of H_2O_2 or auto-decomposition of H_2O_2.[44,45] The redox potential of **2** was higher than that of the enzymatic iron-site, making **2** more prone to reduction.[53] At this time, we are not sure about the source of another electron; however, we are currently exploring various NO_2^- bound $Cu^{I/II}$ & $Fe^{II/III}$ complexes to understand the reaction sequences and track the electron source using the known electron donor species. These results provide entirely new reaction sequences for acid-induced NO_2^- reduction chemistry, a functional model of biomimetic NiR chemistry, and show how the H^+ ion concentration determines H_2O_2 or H_2O as a side product along with NO.

Experimental Section

For the experimental details, see the ESI.†

Data availability

All the required data is already provided in the ESI† and manuscript.

Author contributions

PKK discovered /conceptualized the initial project. Kulbir carried out most of the experiments and gathered the data. PKK, SG & TD helped in interpreting the experimental results. SCS, Kulbir & SD worked on growing the crystals and recording the crystallographic data. Kulbir and SD write the first draft of the article. PKK & TD have corrected the manuscript, finalized the final draft, and guided during the revision. PKK followed and guided the whole project work.

Conflicts of interest

There are no conflicts to declare.

Acknowledgements

This work was supported by a grants-in-aid (Grant No. CRG/2021/003371, & EEQ/2021/000109) from SERB-DST and AvH (ID: 1219648). Kulbir and S. D. thank IISER Tirupati for their fellowship.

References

1 (*a*) R. F. Furchgott, *Angew. Chem., Int. Ed.*, 1999, **38**, 1870–1880; (*b*) L. J. Ignarro, *Angew. Chem., Int. Ed.*, 1999, **38**, 1882–1892; (*c*) L. J. Ignarro, *Nitric Oxide: Biology and Pathobiology*, Academic press, 2000; (*d*) G. B. Richter-Addo, P. Legzdins and J. Burstyn, *Chem. Rev.*, 2002, **102**, 857–860;

(*e*) I. M. Wasser, S. de Vries, P. Moënne-Loccoz, I. Schröder and K. D. Karlin, *Chem. Rev.*, 2002, **102**, 1201–1234.

2 R. B. S. Nabi, R. Tayade, A. Hussain, K. P. Kulkarni, Q. M. Imran, B. G. Mun and B. W. Yun, *Environ. Exp. Bot.*, 2019, **161**, 120–133.

3 F. Vargas, J. M. Moreno, R. Wangensteen, I. Rodriguez-Gomez and J. Garcia-Estan, *Eur. J. Endocrinol.*, 2007, **156**, 1–12.

4 (*a*) H. T. Dong, S. Camarena, D. Sil, M. O. Lengel, J. Zhao, M. Y. Hu, E. E. Alp, C. Krebs and N. Lehnert, *J. Am. Chem. Soc.*, 2022, **144**, 16395–16409; (*b*) D. J. Stuehr, S. S. Gross, I. Sakuma, R. Levi and C. F. Nathan, *J. Exp. Med.*, 1989, **169**, 1011–1020.

5 (*a*) R. E. Huie and S. Padmaja, *Free Radical Res. Commun.*, 1993, **18**, 195–199; (*b*) P. Pacher, J. S. Beckman and L. Liaudet, *Physiol. Rev.*, 2007, **87**, 315–424; (*c*) C. Prolo, M. N. Alvarez and R. Radi, *Biofactors*, 2014, **40**, 215–225.

6 (*a*) W. C. Nottingham and J. R. Sutter, *Int. J. Chem. Kinet.*, 1986, **18**, 1289–1302; (*b*) C. H. Lim, P. C. Dedon and W. M. Deen, *Chem. Res. Toxicol.*, 2008, **21**, 2134–2147.

7 (*a*) R. Radi, *Proc. Natl. Acad. Sci. U. S. A.*, 2004, **101**, 4003–4008; (*b*) B. Kalyanaraman, *Proc. Natl. Acad. Sci. U. S. A.*, 2004, **101**, 11527–11528; (*c*) P. C. Dedon and S. R. Tannenbaum, *Arch. Biochem. Biophys.*, 2004, **423**, 12–22.

8 (*a*) N. Lehnert, T. C. Berto, M. G. I. Galinato and L. E. Goodrich, in *Handbook of Porphyrin Science*, ed. K. Kadish, K. Smith and R. Guilard, World Scientific Publishing, Singapore, 2011, p. 1; (*b*) T. B. McCall, N. K. Boughton-Smith, R. M. Palmer, B. J. Whittle and S. Moncada, *Biochem. J.*, 1989, **261**, 293–296; (*c*) R. G. Knowles and S. Moncada, *Biochem. J.*, 1994, **298**(Pt 2), 249–258.

9 (*a*) B. A. Averill, *Chem. Rev.*, 1996, **96**, 2951–2964; (*b*) E. I. Tocheva, F. I. Rosell, A. G. Mauk and M. E. Murphy, *Science*, 2004, **304**, 867–870.

10 L. Ma, L. Hu, X. Feng and S. Wang, *Aging Dis.*, 2018, **9**, 938–945.

11 (*a*) P. C. Ford and I. M. Lorkovic, *Chem. Rev.*, 2002, **102**, 993–1018; (*b*) M. P. Schopfer, B. Mondal, D. H. Lee, A. A. Sarjeant and K. D. Karlin, *J. Am. Chem. Soc.*, 2009, **131**, 11304–11305; (*c*) M. P. Doyle and J. W. Hoekstra, *J. Inorg. Biochem.*, 1981, **14**, 351–358; (*d*) M. Yenuganti, S. Das, K. Kulbir, S. Ghosh, P. Bhardwaj, S. S. Pawar, S. C. Sahoo and P. Kumar, *Inorg. Chem. Front.*, 2020, **7**, 4872–4882.

12 (*a*) E. Weitzberg and J. O. Lundberg, *Nitric Oxide – Biol. Chem.*, 1998, **2**, 1–7; (*b*) J. O. Lundberg and M. Govoni, *Free Radical Biol. Med.*, 2004, **37**, 395–400.

13 (*a*) L. I. Hochstein and G. A. Tomlinson, *Annu. Rev. Microbiol.*, 1988, **42**, 231–261; (*b*) W. H. Campbell, *Annu. Rev. Plant Physiol. Plant Mol. Biol.*, 1999, **50**, 277–303.

14 P. Tavares, A. S. Pereira, J. J. Moura and I. Moura, *J. Inorg. Biochem.*, 2006, **100**, 2087–2100.

15 N. Lehnert, E. Kim, H. T. Dong, J. B. Harland, A. P. Hunt, E. C. Manickas, K. M. Oakley, J. Pham, G. C. Reed and V. S. Alfaro, *Chem. Rev.*, 2021, **121**, 14682–14905.

16 N. Benjamin, F. O'Driscoll, H. Dougall, C. Duncan, L. Smith, M. Golden and H. McKenzie, *Nature*, 1994, **368**, 502.

17 J. O. Lundberg, E. Weitzberg, J. M. Lundberg and K. Alving, *Gut*, 1994, **35**, 1543–1546.

18 (*a*) S. Kundu, W. Y. Kim, J. A. Bertke and T. H. Warren, *J. Am. Chem. Soc.*, 2017, **139**, 1045–1048; (*b*) K. Cosby, K. S. Partovi, J. H. Crawford, R. P. Patel, C. D. Reiter, S. Martyr, B. K. Yang, M. A. Waclawiw, G. Zalos, X. Xu, K. T. Huang, H. Shields, D. B. Kim-Shapiro, A. N. Schechter, R. O. Cannon and M. T. Gladwin, *Nat. Med.*, 2003, **9**, 1498–1505; (*c*) U. B. Hendgen-Cotta, M. W. Merx, S. Shiva, J. Schmitz, S. Becher, J. P. Klare, H.-J. Steinhoff, A. Goedecke, J. Schrader, M. T. Gladwin, M. Kelm and T. Rassaf, *Proc. Natl. Acad. Sci. U. S. A.*, 2008, **105**, 10256–10261.

19 J. Brooks and D. Keilin, *Proc. R. Soc. London, Ser. B*, 1937, **123**, 368–382.

20 M. Kumar, N. A. Dixon, A. C. Merkle, M. Zeller, N. Lehnert and E. T. Papish, *Inorg. Chem.*, 2012, **51**, 7004–7006.

21 (*a*) S. Hematian, M. A. Siegler and K. D. Karlin, *J. Am. Chem. Soc.*, 2012, **134**, 18912–18915; (*b*) S. Hematian, I. Kenkel, T. E. Shubina, M. Dürr, J. J. Liu, M. A. Siegler, I. Ivanovic-Burmazovic and K. D. Karlin, *J. Am. Chem. Soc.*, 2015, **137**, 6602–6615.

22 M. E. Murphy, S. Turley and E. T. Adman, *J. Biol. Chem.*, 1997, **272**, 28455–28460.

23 R. C. Maji, S. K. Barman, S. Roy, S. K. Chatterjee, F. L. Bowles, M. M. Olmstead and A. K. Patra, *Inorg. Chem.*, 2013, **52**, 11084–11095.

24 A. P. Hunt, A. E. Batka, M. Hosseinzadeh, J. D. Gregory, H. K. Haque, H. Ren, M. E. Meyerhoff and N. Lehnert, *ACS Catal.*, 2019, **9**, 7746–7758.

25 T. S. Kurtikyan, A. A. Hovhannisyan, A. V. Iretskii and P. C. Ford, *Inorg. Chem.*, 2009, **48**, 11236–11241.

26 (*a*) B. C. Sanders, S. M. Hassan and T. C. Harrop, *J. Am. Chem. Soc.*, 2014, **136**, 10230–10233; (*b*) S. Zhang, M. M. Melzer, S. N. Sen, N. Celebi-Olcum and T. H. Warren, *Nat. Chem.*, 2016, **8**, 663–669.

27 (*a*) L. Cheng, D. R. Powell, M. A. Khan and G. B. Richter-Addo, *Chem. Commun.*, 2000, 2301–2302, DOI: **10.1039/B006775J**; (*b*) A. K. Patra, R. K. Afshar, J. M. Rowland, M. M. Olmstead and P. K. Mascharak, *Angew. Chem., Int. Ed. Engl.*, 2003, **42**, 4517–4521.

28 K. Kulbir, S. Das, T. Devi, M. Goswami, M. Yenuganti, P. Bhardwaj, S. Ghosh, S. C. Sahoo and P. Kumar, *Chem. Sci.*, 2021, **12**, 10605–10612.

29 S. Hong, J. J. Yan, D. G. Karmalkar, K. D. Sutherlin, J. Kim, Y. M. Lee, Y. Goo, P. K. Mascharak, B. Hedman, K. O. Hodgson, K. D. Karlin, E. I. Solomon and W. Nam, *Chem. Sci.*, 2018, **9**, 6952–6960.

30 (*a*) J. Heinecke and P. C. Ford, *Coord. Chem. Rev.*, 2010, **254**, 235–247; (*b*) S. Das, K. Kulbir, S. Ghosh, S. Chandra Sahoo and P. Kumar, *Chem. Sci.*, 2020, **11**, 5037–5042; (*c*) S. Das, K. Kulbir, S. Ray, T. Devi, S. Ghosh, S. S. Harmalkar, S. N. Dhuri, P. Mondal and P. Kumar, *Chem. Sci.*, 2022, **13**, 1706–1714.

31 (*a*) A. P. Hunt and N. Lehnert, *Acc. Chem. Res.*, 2015, **48**, 2117–2125; (*b*) A. L. Speelman, B. Zhang, C. Krebs and N. Lehnert, *Angew. Chem., Int. Ed.*, 2016, **55**, 6685–6688.

32 (*a*) P. Kumar, Y. M. Lee, Y. J. Park, M. A. Siegler, K. D. Karlin and W. Nam, *J. Am. Chem. Soc.*, 2015, **137**, 4284–4287; (*b*) P. Kumar, Y. M. Lee, L. Hu, J. Chen, Y. J. Park, J. Yao, H. Chen, K. D. Karlin and W. Nam, *J. Am. Chem. Soc.*, 2016, **138**, 7753–7762; (*c*) S. Hong, J. J. Yan, D. G. Karmalkar, K. D. Sutherlin, J. Kim, Y. M. Lee, Y. Goo, P. K. Mascharak, B. Hedman, K. O. Hodgson, K. D. Karlin, E. I. Solomon and W. Nam, *Chem. Sci.*, 2018, **9**, 6952–6960.

33 (*a*) J. L. Heinecke, C. Khin, J. C. Pereira, S. A. Suarez, A. V. Iretskii, F. Doctorovich and P. C. Ford, *J. Am. Chem. Soc.*, 2013, **135**, 4007–4017; (*b*) T. S. Kurtikyan, A. A. Hovhannisyan and P. C. Ford, *Inorg. Chem.*, 2016, **55**, 9517–9520.

34 (*a*) B. A. Averill, *Chem. Rev.*, 1996, **96**, 2951–2964; (*b*) M. A. Puthiyaveetil Yoosaf, S. Ghosh, Y. Narayan, M. Yadav, S. C. Sahoo and P. Kumar, *Dalton Trans.*, 2019, **48**, 13916–13920.

35 C. Uyeda and J. C. Peters, *J. Am. Chem. Soc.*, 2013, **135**, 12023–12031.

36 W. M. Ching, P. P. Chen and C. H. Hung, *Dalton Trans.*, 2017, **46**, 15087–15094.

37 C. H. Hsieh, S. Ding, O. F. Erdem, D. J. Crouthers, T. Liu, C. C. McCrory, W. Lubitz, C. V. Popescu, J. H. Reibenspies, M. B. Hall and M. Y. Darensbourg, *Nat. Commun.*, 2014, **5**, 3684.

38 (*a*) S. Goswami, D. Sen, N. K. Das, H. K. Fun and C. K. Quah, *Chem. Commun.*, 2011, **47**, 9101–9103; (*b*) J. Chen, H. Yoon, Y. M. Lee, M. S. Seo, R. Sarangi, S. Fukuzumi and W. Nam, *Chem. Sci.*, 2015, **6**, 3624–3632; (*c*) Y. M. Lee, M. Yoo, H. Yoon, X. X. Li, W. Nam and S. Fukuzumi, *Chem. Commun.*, 2017, **53**, 9352–9355.

39 (*a*) P. C. Ford, J. C. M. Pereira and K. M. Miranda, in *Nitrosyl Complexes in Inorganic Chemistry, Biochemistry and Medicine II*, ed. D. M. P. Mingos, Springer Berlin Heidelberg, Berlin, Heidelberg, 2014, pp. 12–44, DOI: DOI: 10.1007/430_2013_117; (*b*) G. R. Wyllie and W. R. Scheidt, *Chem. Rev.*, 2002, **102**, 1067–1090; (*c*) D. M. P. Mingos, in *Nitrosyl Complexes in Inorganic Chemistry, Biochemistry and Medicine I*, ed. D. M. P. Mingos, Springer Berlin Heidelberg, Berlin, Heidelberg, 2014, pp. 1–44, DOI: DOI: 10.1007/430_2013_116.

40 (*a*) Y. Li, M. Hodak and J. Bernholc, *Biochemistry*, 2015, **54**, 1233–1242; (*b*) O. Einsle, A. Messerschmidt, R. Huber, P. M. Kroneck and F. Neese, *J. Am. Chem. Soc.*, 2002, **124**, 11737–11745; (*c*) S. Basu, N. A. Azarova, M. D. Font, S. B. King, N. Hogg, M. T. Gladwin, S. Shiva and D. B. Kim-Shapiro, *J. Biol. Chem.*, 2008, **283**, 32590–32597; (*d*) S. Besson, C. Carneiro, J. J. Moura, I. Moura and G. Fauque, *Anaerobe*, 1995, **1**, 219–226; (*e*) M. J. Boulanger, M. Kukimoto, M. Nishiyama, S. Horinouchi and M. E. Murphy, *J. Biol. Chem.*, 2000, **275**, 23957–23964; (*f*) J. Brooks and D. Keilin, *Proc. R. Soc. London, Ser. B*, 1937, **123**, 368–382; (*g*) S. L. Rose, S. V. Antonyuk, D. Sasaki, K. Yamashita, K. Hirata, G. Ueno, H. Ago, R. R. Eady, T. Tosha, M. Yamamoto and S. S. Hasnain, *Sci. Adv.*, 2021, **7**, eabd8523; (*h*) M. Kujime and H. Fujii, *Angew. Chem., Int. Ed. Engl.*, 2006, **45**, 1089–1092; (*i*) S. Maekawa, T. Matsui, K. Hirao and Y. Shigeta, *J. Phys. Chem. B*, 2015, **119**, 5392–5403; (*j*) S. C. Hsu, Y. L. Chang, W. J. Chuang, H. Y. Chen, I. J. Lin, M. Y. Chiang, C. L. Kao and H. Y. Chen, *Inorg. Chem.*, 2012, **51**, 9297–9308.

41 M. Lintuluoto and J. M. Lintuluoto, *Metallomics*, 2018, **10**, 565–578.

42 (*a*) B. Chen, Y. Xia, R. He, H. Sang, W. Zhang, J. Li, L. Chen, P. Wang, S. Guo, Y. Yin, L. Hu, M. Song, Y. Liang, Y. Wang, G. Jiang and R. N. Zare, *Proc. Natl. Acad. Sci. U. S. A.*, 2022, **119**, e2209056119; (*b*) P. Ulanski and C. von Sonntag, *J. Chem. Soc., Perkin Trans. 2*, 1999, 165–168, DOI: 10.1039/a808543i.

43 J. A. Halfen, S. Mahapatra, E. C. Wilkinson, A. J. Gengenbach, V. G. Young, L. Que and W. B. Tolman, *J. Am. Chem. Soc.*, 1996, **118**, 763–776.

44 (*a*) B. Mlasi, D. Glasser and D. Hildebrandt, *Ind. Eng. Chem. Res.*, 2015, **54**, 5589–5597; (*b*) F. M. Fomin and K. S. Zaitseva, *Russ. J. Phys. Chem. A*, 2014, **88**, 466–470.

45 P. Pędziwiatr, F. Mikołajczyk, D. Zawadzki, K. Mikołajczyk and A. Bedka, *Acta Innov.*, 2018, 45–52, DOI: 10.32933/ActaInnovations.26.5.

46 N. A. Stephenson and A. T. Bell, *Anal. Bioanal. Chem.*, 2005, **381**, 1289–1293.

47 K. Mase, K. Ohkubo, Z. Xue, H. Yamada and S. Fukuzumi, *Chem. Sci.*, 2015, **6**, 6496–6504.

48 (*a*) Z. H. L. Abraham, B. E. Smith, B. D. Howes, D. J. Lowe and R. R. Eady, *Biochem. J.*, 1997, **324**, 511–516; (*b*) Z. Huang, S. Shiva, D. B. Kim-Shapiro, R. P. Patel, L. A. Ringwood, C. E. Irby, K. T. Huang, C. Ho, N. Hogg, A. N. Schechter and M. T. Gladwin, *J. Clin. Invest.*, 2005, **115**, 2099–2107; (*c*) C. A. Clark, C. P. Reddy, H. Xu, K. N. Heck, G. H. Luo, T. P. Senftle and M. S. Wong, *ACS Catal.*, 2020, **10**, 494–509; (*d*) H.-Y. Hu, N. Goto and K. Fujie, *Water Res.*, 2001, **35**, 2789–2793.

49 (*a*) A. Samouilov, P. Kuppusamy and J. L. Zweier, *Arch. Biochem. Biophys.*, 1998, **357**, 1–7; (*b*) K. Tsuchiya, Y. Kanematsu, M. Yoshizumi, H. Ohnishi, K. Kirima, Y. Izawa, M. Shikishima, T. Ishida, S. Kondo, S. Kagami, Y. Takiguchi and T. Tamaki, *Am. J. Physiol. Heart Circ.*, 2005, **288**, H2163–H2170.

50 A. Dubey, V. Rives and S. Kannan, *J. Mol. Catal. A: Chem.*, 2002, **181**, 151–160.

51 (*a*) A. Arnold, R. Metzinger and C. Limberg, *Chemistry*, 2015, **21**, 1198–1207; (*b*) C. Citek, C. T. Lyons, E. C. Wasinger and T. D. Stack, *Nat. Chem.*, 2012, **4**, 317–322; (*c*) P. T. Kaye, K. W. Wellington and G. M. Watkins, *Arkivoc*, 2010, **2009**, 301–313.

52 S. Suzuki, K. Kataoka and K. Yamaguchi, *Acc. Chem. Res.*, 2000, **33**, 728–735.

53 C. E. Immoos, J. Chou, M. Bayachou, E. Blair, J. Greaves and P. J. Farmer, *J. Am. Chem. Soc.*, 2004, **126**, 4934–4942.